National Conference with International Participation
ENGINEERING MECHANICS 2003
Svratka, Czech Republic, May 12 – 15, 2003
paper no. 257

VISCO-PLASTIC MODEL WITH TIME RETARDATION FOR HIGH-VELOCITY IMPACT LOADING OF OFE COPPER SPECIMENS

J. Plešek*, E. Hirsch†

Summary: *OFE copper (Oxygen Free Electronic copper) is extensively used in military engineering for the design of shape charge warheads. Use is made of its excellent deformation capabilities to initiate a metal jet for the target penetration moving with the speed of several kilometers per second. Gray and Follansbee (1988) conducted unique experiments with OFE copper specimens subject to such extreme loading conditions. Controversial results were obtained that could not be explained by any existing visco-plastic theory. The authors of this paper made an attempt at an explanation by introducing a specific visco-plastic model with time retardation. In the present work the model was cast to the format of the standard continuum mechanics equations.*

1. Introduction

A visco-plastic model involving time delay caused by internal material's structure inertia was proposed by Hirsch and Plešek (2003). Its uniaxial representation derived from experimental data measured by Gray and Follansbee (1988) under high-velocity impact conditions can be summarized as follows.

A material subject to shock loadings highly exceeding its yield stress cannot immediately release the elastic strain energy accumulated upon the shock rise-time. Macroscopic plastic flow smeared over material grains is delayed according to the approximate formula

$$\left(\frac{\sigma_e}{2G}\right)^{3/2} \tau = \tau_0 = const. \tag{1}$$

Here, σ_e is the effective stress, G the shear modulus and τ is the retardation time measuring the delay between the arrival of a shock wave and the initiation of macroscopic yielding. The material constant τ_0 on the right-hand side of the equation is called the intrinsic time of the material. In order to put the above observations in a formal context and derive quantitative results the problem is rephrased in terms of continuum mechanics equations.

*Jiří Plešek, Institute of Thermomechanics, Academy of Sciences of the Czech Republic; Dolejškova 5; 182 00 Praha 8; e-mail: plesek@it.cas.cz

†Eitan Hirsch, IDF, MIL P.O.BOX 01055, Israel

Total strain ϵ_x is computed from the Hugoniot curve according to the applied shock load pressure P, which corresponds to the assumption that the bulk modulus is a function of hydrostatic pressure. On the other hand, the shear modulus G will be little influenced by P, therefore, G is assumed to retain its initial value as in linear elasticity theory. Hooke's law then implies

$$\sigma_x - \sigma_r = 2G(\epsilon_x^e - \epsilon_r^e) \tag{2}$$

The von Mises effective stress under uniaxial strain is defined as

$$\sigma_e = |\sigma_x - \sigma_r| = 2G|\epsilon_x^e - \epsilon_r^e| \tag{3}$$

With respect to plastic yielding the material is incompressible

$$\epsilon_x^p + \epsilon_r^p + \epsilon_r^p = 0 \tag{4}$$

therefore $\epsilon_r^p = -\frac{1}{2}\epsilon_x^p$. In the radial direction $\epsilon_r = \epsilon_r^e + \epsilon_r^p = 0$ hence $\epsilon_r^e = \frac{1}{2}\epsilon_x^p$ and in the x-direction $\epsilon_x = \epsilon_x^e + \epsilon_x^p$. Substituting these results to Eq. (3) we arrive at

$$\sigma_e = 2G|\epsilon_x - \tfrac{3}{2}\epsilon_x^p| \tag{5}$$

The last equation suggests that the plastic strain can never exceed the critical value that would have reduced the effective stress to zero. Thus

$$|\epsilon_x^p| \leq \tfrac{2}{3}|\epsilon_x| \tag{6}$$

and $\frac{2}{3}|\epsilon_x|$ may be thought of as an upper limit for plastic strain in the course of relaxation process. Obviously, the actual plastic strain will be much smaller due to viscous effects, which is discussed next.

2. Viscoplastic model

The simplest rate dependent constitutive equation to be used with rather limited experimental data is Perzyna's (1963) overstress model

$$\dot{\epsilon}_p = \gamma \left(\frac{\sigma_e - \sigma_Y}{\sigma_Y} \right)^m \tag{7}$$

where γ, m are material constants, σ_Y is the subsequent yield stress of the material hardened by the shock passage, $\sigma_e > \sigma_Y$, and $\dot{\epsilon}_p$ is the rate of the equivalent plastic strain

$$\dot{\epsilon}_p = \sqrt{\tfrac{2}{3}\dot{\epsilon}_{ij}^p \dot{\epsilon}_{ij}^p} = |\dot{\epsilon}_x^p| \tag{8}$$

The incompressibility condition Eq. (4) was used to simplify the last definition. Now, Eq. (5), (8) are inserted into Eq. (7) after which the differential equation is obtained

$$\dot{\epsilon}^p = \gamma \left(\frac{2G(\epsilon - \frac{3}{2}\epsilon^p) - \sigma_Y}{\sigma_Y} \right)^m \tag{9}$$

where $-\epsilon_x^p = \epsilon^p \geq 0$ and $-\epsilon_x = \epsilon > 0$ for compression loading were used for simplicity.

The governing differential equation of the relaxation process $\epsilon = const.$ can be integrated with the initial condition $\epsilon^p(\tau) = 0$ to get

$$\left(\frac{2G}{\sigma_Y}(\epsilon - \frac{3}{2}\epsilon^p) - 1\right)^{1-m} - \left(\frac{2G}{\sigma_Y}\epsilon - 1\right)^{1-m} = (m-1)\frac{3G}{\sigma_Y}\gamma(t-\tau) \tag{10}$$

where $t - \tau$ is the pulse duration after the retardation time τ has elapsed and $m > 1$. For $m = 1$ we get instead of Eq. (10) the expression

$$\epsilon^p = (\frac{2}{3}\epsilon - \frac{\sigma_Y}{3G})(1 - \exp\Big[-\frac{3G}{\sigma_Y}\gamma(t-\tau)\Big]) \tag{11}$$

3. Identification of material parameters

At least, two sets of measurements for substitution to Eq. (10) must be available to calibrate m and γ. Given the data by Gray and Follansbee (1988) the measurements of permanent deformation were difficult to carry out with sufficient accuracy. Thus, the only information found in the paper was that the permanent strain did not exceed 1.5%.

The best way to start with, under such circumstances, is to make an idea how sensitive the solution is to the choice of m parameter. Using the values $G = 47$ GPa, $\sigma_Y = 200$ MPa and the values of ϵ—taken from experiments by Gray and Follansbee (1988)—we can obtain the characteristics of ϵ^p since the end of the retardation time till the rarefaction has arrived. For the 20 GPa shock load, the plot of ϵ^p against dimensionless time $\gamma(t-\tau)$ shown in Fig. 1 is obtained.

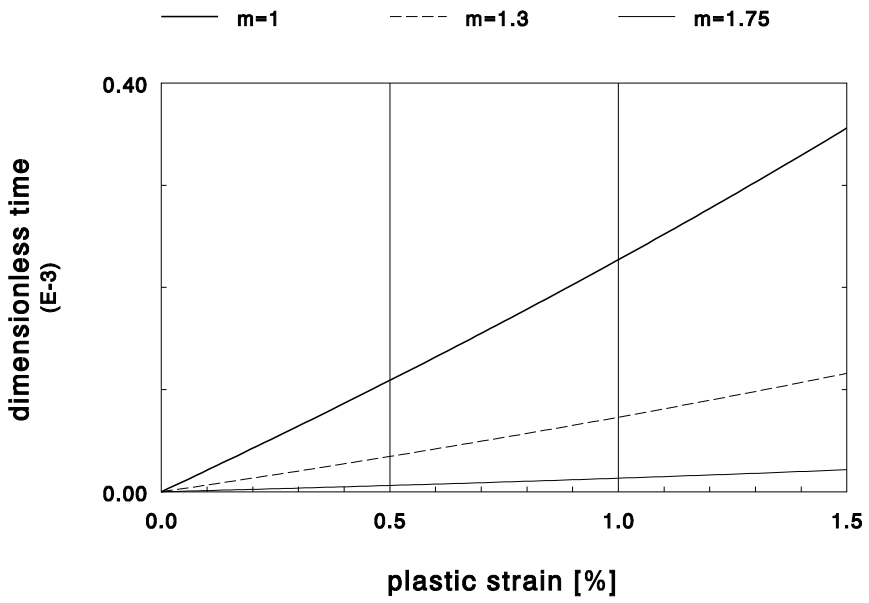

Figure 1: Numerical solution of Eq. (9) at constant strain.

The stress exponent m strongly influences the amount of plastic strain predicted at a fixed time but the characteristics remain nearly straight lines up to 1.5% deformation regardless of the (reasonable) m value. It follows that plastic yielding occurs at roughly constant stress and the differential equation Eq. (9) can be solved approximately as

$$\epsilon_i^p \simeq \gamma \left(\frac{2G\epsilon_i - \sigma_{Yi}}{\sigma_{Yi}} \right)^m (t_i - \tau_i) \tag{12}$$

where subscript i refers to a particular experiment. Upon elimination of γ from Eq. (12) the m-parameter is expressed as a function of the ratio $\epsilon_i^p/\epsilon_j^p$ for two independent measurements i and j. In this way, the demand for accurate data can be substantially relaxed by requiring only the knowledge of the two plastic strains ratio rather than their total magnitudes.

In the present work even this datum is unavailable, therefore, the stress exponent cannot be determined. On the other hand, if we confine ourselves to the modelling of experiments under fixed loading level the solution is little sensitive to m. This parameter may then be set arbitrarily provided that a proper choice of γ has been made. In other words, only one independent parameter needs to be identified for a short pulse analysis at a given impact velocity.

If, for instance, the 20 GPa shock load is considered the exact solution Eq. (10) can be used to compute fludity parameter γ taking the plastic strain measured at its upper limit $\epsilon^p = 0.015$. Any of the matching pairs m, γ listed in Tab. 1 can be substituted as an input to a computer code to predict about the same elastic-viscoplastic response for the stress level given. Of course, much more accurate experiments would have to be carried out in order to decide which of the pairs provides the closest fit.

Table 1: Matching values of material parameters.

m	1	2	3	4	5
γ [1/s]	1047	25.0	0.599	0.0144	3.50×10^{-4}

4. Inclusion of intrinsic time via internal variable

It is impractical to use the retardation model in numerical analyses in the fashion presented so far since it would be difficult to handle τ within the context of internal state variable formalism. In this section, we rephrase the model to a more suitable form.

A general expression for visco-plastic constitutive equations can be written as

$$\dot{\boldsymbol{\epsilon}}^p = \frac{3}{2} \frac{\dot{\epsilon}_p}{\sigma_e} \mathbf{S} \tag{13}$$

in which $\dot{\boldsymbol{\epsilon}}^p$ is the visco-plastic strain tensor and $\mathbf{S}$ is the deviatoric stress. Eq.(7) is modified to

$$\dot{\epsilon}_p = \bar{\gamma} \left(\frac{\sigma_e - \sigma_Y}{\sigma_Y} \right)^m H(\sigma_e - \sigma_Y) \tag{14}$$

where H denotes the Heaviside step function and $\bar{\gamma}$ is considered to be dependent on equivalent plastic strain ϵ_p. In principle, other internal variables such as backstress may amend the system to invoke more complex hardening laws.

Now, the question is how to enforce the material reponse plotted schematically in Fig. 2a. Theoretically, the plastic strain should be zero in interval $[0, \tau]$, which is impossible to achieve if $\bar{\gamma}$ is supposed to be a function of standard internal variables (but not the explicit function of time). It may be feasible, on the other hand, to approximate this zero function by small values varying between the user defined limits ϵ_{p0} and $\epsilon_{p\tau}$. These limits are bound to maintain sufficient numerical accuracy.

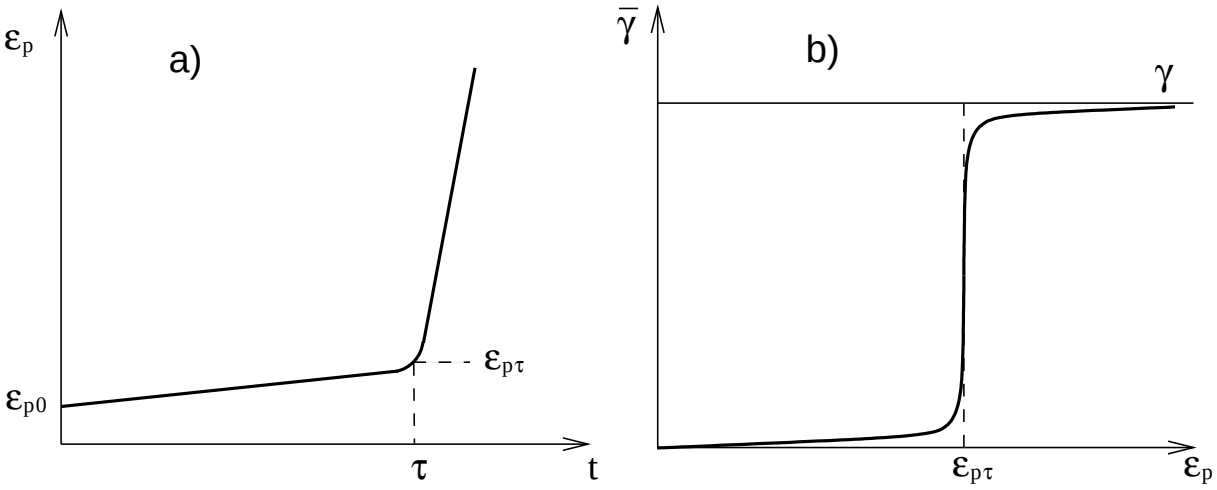

Figure 2: Schematic plot of the hardening function $\bar{\gamma}$.

An analytical function satisfying such requirements reads

$$\bar{\gamma}(\epsilon_p) = \frac{\gamma \epsilon_p^n}{\epsilon_{p\tau}^n + \epsilon_p^n} \tag{15}$$

where γ is the same constant as in Eq. (7) and n is a large number controlling the abruptness of the jump at $\epsilon_{p\tau}$ in Fig. 2b. Solution of Eq. (14) at constant stress leads to

$$\epsilon_p^n - \epsilon_{p0}^n + \frac{\epsilon_{p\tau}^n}{(n-1)\epsilon_{p0}^{n-1}} - \frac{\epsilon_{p\tau}^n}{(n-1)\epsilon_p^{n-1}} = \gamma \left(\frac{\sigma_e - \sigma_Y}{\sigma_Y} \right)^m t \tag{16}$$

Substituting $t = \tau$ and defining $\epsilon_{p0} = \alpha \epsilon_{p\tau}$, $\alpha < 1$ we have

$$(1 - \alpha^n)\epsilon_{p\tau}^n + \frac{\epsilon_{p\tau}}{(n-1)\alpha^{n-1}} = \gamma \left(\frac{\sigma_e - \sigma_Y}{\sigma_Y} \right)^m \tau + \frac{\epsilon_{p\tau}^n}{n-1} \tag{17}$$

The last relation should be understood as a condition on numerical parameters $\epsilon_{p\tau}$, α and n so that the turning point in Fig. 2a was placed exactly at time τ. For $\epsilon_{p\tau}$ being small and n large the approximate solution for α is

$$\alpha \simeq \left[(n-1) \frac{\gamma}{\epsilon_{p\tau}} \left(\frac{\sigma_e - \sigma_Y}{\sigma_Y} \right)^m \tau \right]^{\frac{1}{1-n}} \tag{18}$$

For chosen $\epsilon_{p\tau}$, n one can compute α from Eq. (18) and $\epsilon_{p0} = \alpha\epsilon_{p\tau}$ at each time step in a numerical analysis. If $\epsilon_{p0} > \epsilon_p(t)$ then the threshold ϵ_{p0} is inserted to Eq. (15) for integration; otherwise the current value $\epsilon_p(t)$ should be used. According to Eq. (1), τ is treated as a function of σ_e in problems with varying stress.

The described material model can now be completed by elastic relations of the type

$$\boldsymbol{\sigma} = \mathbf{C} :(\boldsymbol{\epsilon} - \boldsymbol{\epsilon}^p) \tag{19}$$

in which the fourth order tensor $\mathbf{C}$ has the isotropic structure

$$C_{ijkl} = (K - \tfrac{2}{3}G)\delta_{ij}\delta_{kl} + G(\delta_{ik}\delta_{jl} + \delta_{il}\delta_{jk}) \tag{20}$$

As already mentioned, in the latter expression the shear modulus G is supposed to be constant, i.e. $G = G_0$, whereas the bulk modulus K is rendered dependent on its initial value K_0 and the hydrostatic pressure P.

An appropriate function can be derived from Hugoniot's equations as

$$\bar{K} = \frac{K_0}{2} + sP + \sqrt{\left(\frac{K_0}{2}\right)^2 + sK_0P} \tag{21}$$

where $\bar{K}$ is the secant bulk modulus defining the bulk sound speed and s is Hugoniot's material constant; $s = 1.489$ for copper. The dependence $P(\theta)$ generated by Eqs. (20) and (19) must be such that

$$\frac{\mathrm{d}P}{\mathrm{d}\theta} = \bar{K} \ , \quad \theta = \mathrm{tr}(\boldsymbol{\epsilon} - \boldsymbol{\epsilon}^p) \tag{22}$$

Thus $K \to K_0$ as one of the parameters s or P approaches zero.

In this form, the proposed model with retardation time can be easily implemented in any existing finite element code since the required modifications merely consist in Eq. (21) and Eq. (15) together with Eq. (18) that describe simple hardening behaviour.

5. Numerical example

As an example, consider the 20 GPa shock data, i.e. $\sigma_e = 2G\epsilon = 9.729$ GPa, $t = 1$ μs, $\sigma_Y = 0.2$ GPa, $\tau = 0.66$ μs after Gray and Follansbee (1988) and m, γ are determined according to Tab. 1.

We started with the investigation of the material model sensitivity to the choice of numerical parameters n and $\epsilon_{p\tau}$. Eq. (15) can be cast to the form

$$\frac{\bar{\gamma}(\epsilon_p)}{\gamma} = \frac{(\epsilon_p/\epsilon_{p\tau})^n}{1 + (\epsilon_p/\epsilon_{p\tau})^n} \tag{23}$$

which suggests that arbitrary units can be used for $\bar{\gamma}$ and ϵ_p. Fig. 3 shows this function with $\gamma = 1$, $\epsilon_{p\tau} = 1$ for increasing values of the n-exponent.

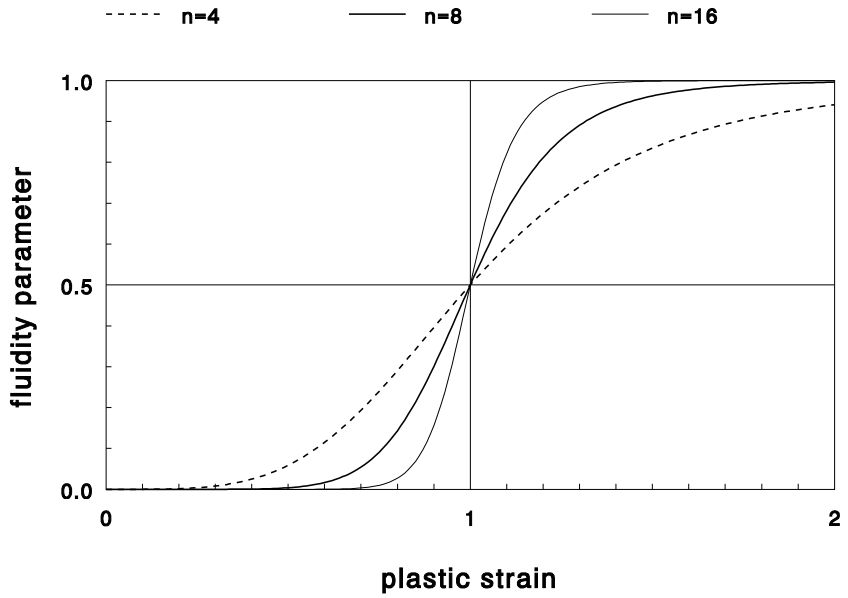

Figure 3: Sensitivity of the hardening function to curvature exponent n.

At first glance, the S-shape curves do not represent well the desired step-wise characteristics for small n up to about $n \simeq 16$. Moreover, the higher this exponent the higher the probability of incurring numerical instabilities in the integration process. Fortunately, $\epsilon_p(t)$ solution plotted in Fig. 4 also depends on the threshold value $\epsilon_{p\tau}$, which to a large extent supresses the influence of n. The legend numbers in Fig. 4 denote first the threshold value, the second introduced by a comma is n. A perfect agreement between the numerical solution and the theoretical model, composed of the zero axis in interval $[0, \tau]$ and the straight line with slope $\gamma = const.$ afterwards, wittnesses a considerable robustness of the proposed analytical expression. Safe inputs $n = 8$, $\epsilon_{p\tau} = 10^{-6}$ thus may be recommended in most situations.

It should be noted that the plastic strain at the end time 1 μs overshoots the prescribed value $\epsilon_p = 1.5\%$. This is because the integration was performed at constant stress whereas the material parameters m, γ were fit using the exact solution of Eq. (10) that took into account stress relaxation. This deviation can be hardly seen in the scale of Fig. 1 where all the curves look like straight lines.

In order to verify the model's response under varying stress conditions the differential equation Eq. (9) with $\bar{\gamma}$ replacing the former constant γ was solved. Numerical computations were carried out for all the matching values in Tab. 1 with input parameters $n = 8$, $\epsilon_{p\tau} = 10^{-6}$ substituted. The results are shown in Fig. 5. It follows, on one hand, that the exact solution Eq. (10) with relaxation effect included must be used to fit material parameters but, on the other hand, once it has been done and matching constants m, γ have been established there is little difference between the cases $m = 1 \div 5$. Thus, in agreement with the discussion in section 3. one may conclude that the infuence of m on the stress change can be disregarded in a short pulse analysis provided a consistent set of material constants is available.

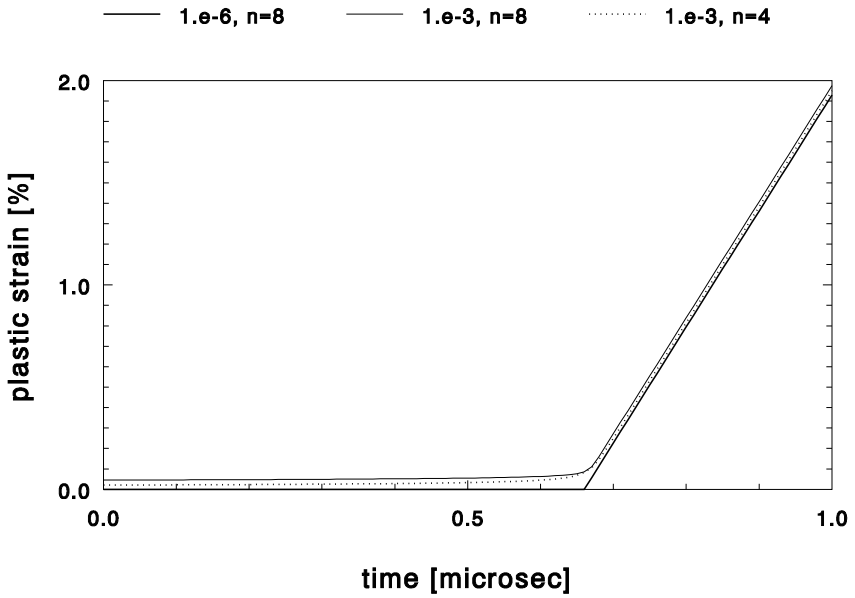

Figure 4: Numerical solution of Eq. (14) at constant stress; $m = 2$.

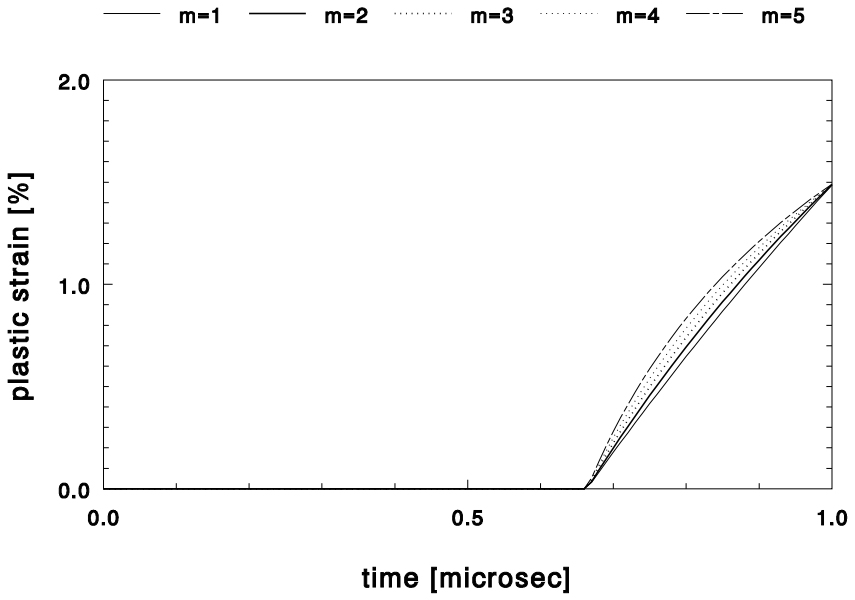

Figure 5: Numerical solution of Eq. (9) at constant strain.

6. Conclusions

Due to the material inertia the formation of a new internal order essential for a plastic slip to take place needs time. This dilation notable in experiments with high-velocity impacted copper specimens was called the retardation time. Its value reduces with an increase of the shock pressure, as expressed by Eq. (1). This type of dependence between the pulse pressure value and its time length is also found in the spallation phenomenon. A similar dependence on the material inertia probably explains such observation.

The mathematical description given above to the observed process is mainly aimed to provide a tool for describing the material response within the context of FE simulations. To obtain a more accurate description of this physical process further detailed investigation will be needed. For example, the length of time of the temporary retardation as a function of the shock pressure needs to be studied in detail. Also the influence of the pressure pulse rise time on the grains break-up process, when this pulse has not yet developed into a shock front, calls for a special study. The outlined procedure for numerical simulation, however, can readily accommodate all such subtleties without the demand for a serious reorganization of a computer code.

7. Acknowledgements

This work was sponsored by the Grant Agency CR under project No. 101/03/0331. The second author was financially supported by the IDF Israel.

8. References

Gray III, G.T. & Follansbee, P.S. (1988) Influence of peak pressure and pulse duration on substructure development and threshold stress measurements in shock loaded copper, in: *Impact Loading and Dynamic Behaviour of Materials*, 2, DCM Informationsgesellschaft Verlag, pp. 541–548.

Hirsch, E. & Plešek, J. (2003) A theoretical analysis of experimental results of very short shock waves load of OFE copper relating the observed metallurgical structure to the deformation mechanism. Submitted to *Int. J. Impact Engng*.

Perzyna, P. (1963) The constitutive equations for rate sensitive plastic materials. *Quart. Appl. Math.*, 20, pp. 321–332.